Available online at www.sciencedirect.com
SCIENCE DIRECT
Continental Shelf Research 24 (2004) 1339–1357
CONTINENTAL SHELF RESEARCH
www.elsevier.com/locate/csr

The freshwater transport and dynamics of the western Maine coastal current

W.R. Geyer[a,*], R.P. Signell[b], D.A. Fong[a], J. Wang[c], D.M. Anderson[a], B.A. Keafer[a]

[a] *Department of Applied Ocean Physics and Engineering, Woods Hole Oceanographic Institution, 384 Woods Hole Road, Woods Hole, MA 02543, USA*
[b] *USGS, 384 Woods Hole Road, Woods Hole, MA 02543-1598, USA*
[c] *International Arctic Research Center, University of Alaska, Fairbanks, USA*

Received 24 July 2002; received in revised form 11 March 2004; accepted 6 April 2004

Abstract

Observations in the Gulf of Maine, USA, were used to characterize the freshwater transport, temporal variability and dynamics of the western Maine coastal current. These observations included moored measurements, multiple hydrographic surveys, and drifter releases during April–July of 1993 and 1994. There is a strong seasonal signal in salinity and along-shore velocity of the coastal current, caused by the freshwater inputs of the rivers entering the western Gulf. Surface salinity within the coastal current during the spring freshet is typically 2 psu below ambient, and along-shore currents in the surface layer are directed southwestward at speeds of 0.10–0.20 m s^{-1}, occasionally reaching 0.50 m s^{-1}. The plume thickness is typically 10–20 m in water depths of 50–100 m, thus it is well isolated from the bottom over most of its areal extent. The along-coast freshwater transport within the plume varies considerably due to variations in wind stress, but on time scales of weeks to months it follows the variations of riverine input, with a time lag consistent with the advective velocity. Less than half of the transport of the coastal current is explained by the baroclinic gradient; the barotropic forcing associated with the larger-scale dynamics of the Gulf of Maine accounts for about 60% of the transport. The volume of freshwater transport in the coastal current exceeds the local riverine input of fresh water by 30%, suggesting a significant contribution of freshwater transport from the St. John River, 500 km northeastward. The measurements within the western Maine coastal current, however, indicate a significant decrease in the baroclinic transport of fresh water along the coast, with an e-folding scale of approximately 200 km.

Keywords: Freshwater; Maine; Coastal current; Measurements

*Corresponding author.
E-mail address: rgeyer@whoi.edu (W.R. Geyer).

0278-4343/$ - see front matter
doi:10.1016/j.csr.2004.04.001

1. Introduction

The freshwater discharge from rivers and estuaries provides an important driving force for the circulation of the coastal ocean. Adjacent to the mouth, the buoyant transport constitutes a river plume (Garvine, 1974; Munchow and Garvine, 1993), in which the momentum from the river or estuary plays a significant part in the dynamics. Farther from the mouth, the influence of the earth's rotation usually causes the buoyant outflow to evolve into a coastal current (Garvine, 1999; Munchow and Garvine, 1993; Chao and Boicourt, 1986), which flows in the direction of Kelvin wave propagation with the shore to the right in the Northern Hemisphere. (Note that in this paper, the terms *plume* and *coastal current* are used to indicate the region of significant salinity anomaly associated with freshwater outflow.) The density anomaly associated with the freshwater outflow is generally assumed to be a major driving force for the propagation of coastal currents; however a number of studies have shown that wind stress is also an important forcing agent on river plumes (Chao, 1988; Muchow and Garvine, 1993; Fong et al., 1997; Kourafalou, 1999; Hickey et al., 1998). Upwelling-favorable winds (opposing the direction of Kelvin wave propagation) cause seaward spreading of the plume and retard or reverse the along-coast motion, whereas downwelling-favorable winds squeeze the plume against the coast and accelerate its down-coast flow. Winds may cause the along-coast transport of fresh water within the coastal current to differ from that being supplied by the river, resulting in either an expansion or collapse of the river plume, as demonstrated in observations of the Amazon plume by Lentz and Limeburner (1995).

Ambient along-shelf currents also influence the transport in coastal currents and may have a pronounced effect on the structure of plumes. Fong and Geyer (2002) performed numerical studies that indicate that in the absence of along-shelf flows, the transport within a coastal current is usually significantly smaller than the riverine supply, leading to a temporally growing bulge at the mouth. Such bulges are commonly observed in numerical model runs (e.g., Chao and Boicourt, 1986; Oey and Mellor, 1993; Kourafalou et al., 1996) and occasionally in observations (Hickey et al., 1998). Fong and Geyer's study indicates that an along-coast flow of as little as $5\,cm\,s^{-1}$ (in the direction of Kelvin wave propagation) augments the transport within the coastal current enough to match the riverine supply and attenuate the growth of the bulge.

Several studies have documented the far-field transport of low-salinity water by coastal currents. Dinnel and Wiseman (1986) showed that fresh water issuing from the Mississippi extended 500 km along the coast. Chapman et al. (1986) indicated that freshwater transport of the Labrador Current from its origin near Baffin Island to the mid-Atlantic bight extends more than 5000 km. Garvine (1999) found, based on numerical studies, that a coastal current like the Delaware outflow would extend on the order of 500 km along-shelf in the absence of external forcing agents, and a larger-scale current with parameters consistent with the Labrador Current would indeed extend more than 7000 miles (not accounting for frictional effects of tides). These calculations require an estimate of vertical eddy viscosity, which is not well constrained by data (Garvine, 1999); nevertheless these numerical studies support the observational result that the along-coast extent of plumes may be very large, particularly with large river outflow and deep receiving waters.

The western Maine coastal current (WMCC) is a buoyant current that flows southwestward around the perimeter of the Gulf of Maine (Bigelow, 1927; Brooks, 1985; Franks and Anderson, 1992; Fong et al., 1997). It is fed by the combined discharge of the Kennebec, Androscoggin, Penobscot and Merrimack Rivers, with a typical annual peak combined discharge of around $7000\,m^3\,s^{-1}$ during the spring freshet (Nielsen et al., 1996). The St. John River discharges a comparable amount to the sum of these rivers (Lynch et al., 1997) into the Bay of Fundy, at the northeastern end of the Gulf of Maine. The St. John outflow feeds into a coastal current in the eastern Gulf, but the current is deflected offshore near the entrance to Penobscot Bay. The observations by Brooks (1985) and Pettigrew et al. (1998) suggest that this current may intermittently return to the coast to feed the WMCC, but the structure appears to be highly variable and observations were not conclusive. Numerical modeling studies by Lynch et al. (1997) based on springtime climatology also indicated the offshore deflection of the coastal current, but they also showed that the depth-integrated transport streamline reattaches to the coast in the western Gulf after being deflected 50 km offshore near Penobscot Bay. The trajectory of the surface waters may differ considerably from the depth-integrated flow, particularly as a function of wind stress, but this model result suggests that the eastern Maine coastal current could contribute to the along-coast freshwater transport in the western Gulf.

An intensive field program was conducted during the springs of 1993 and 1994 to investigate the kinematics and dynamics of the WMCC. This study was part of an interdisciplinary investigation of the influence of physical transport processes on the distribution and fate of the toxic dinoflagellate *Alexandrium tamarensce*, a "red tide" species that contaminates shellfish, causing paralytic shellfish poisoning. However, this paper is limited to the physical aspects of the coastal current transport.

These observations allow a detailed examination of the seasonal development of the plume, with particular attention to the variation in along-coast transport of fresh water due to variations in winds, run-off, and ambient along-coast flow. Time-series measurements were obtained within the coastal current for durations of 3.5 months in 1993 and 7 months in 1994, extending through the rise and fall of the spring freshet. Numerous hydrographic surveys resolved the spatial structure of the plume during different forcing conditions. Fong et al. (1997) used these measurements to investigate the response of the coastal current to variations in wind forcing, noting large variations in the width of the plume as a result of upwelling- and downwelling-favorable winds. This paper focuses on the along-coast, freshwater transport, considering the relative roles of buoyancy and wind forcing, and considering the potential role of the eastern Maine coastal current as a source for fresh water in the WMCC.

2. Field program

The field program consisted of moored, shipboard and drifter measurements in the western Gulf of Maine during the springs of 1993 and 1994. Data were obtained along a 200-km stretch of the Gulf from Penobscot Bay to Cape Cod (Fig. 1), but the central focus of the program was the Cape Porpoise transect, 60 km southwest of the mouth of the Kennebec River.

2.1. Moored measurements

In 1993, moorings were deployed at locations M and P2 (Fig. 1) between March 20 and July 9. These moorings had vector-measuring current meters (VMCMs) at 5-m depths and vector-averaging current meters (VACMs) at 27- and 50-m depths, in water depths of approximately 100 m. All current-meter data was filtered with a 33-h low-pass filter to remove tides and inertial motions. Temperature and conductivity were measured at the same depths as the velocities with Seabird sensors. The M mooring provided data upstream (relative to the ambient, along-coast flow) of the mouth of the Kennebec River. The P2 mooring was intended to provide data within and beneath the Kennebec plume, although sometimes the plume was inshore of the mooring.

In 1994, moorings were deployed at locations K, P1, P2 and S (Fig. 1), between February 17 and October 13. K, P2 and S moorings were close to the 100-m isobath and P1 was close to the 50-m isobath. The three deeper moorings had the same vertical distribution of sensors as the 1993 moorings; the P1 mooring had sensors only at 5 and 27 m. The K mooring provided data in the vicinity of the mouth of the Kennebec River, and P1 and P2 provided improved resolution of the plume relative to the 1993 observations. Currents were rotated into along-shore and cross-shore components, based on the local trend of the bathymetry.

The near-surface current measurements obtained by the VMCMs during both 1993 and 1994 showed a persistent offshore component of flow that is believed to be due to a systematic error in the compasses due to interference by the battery

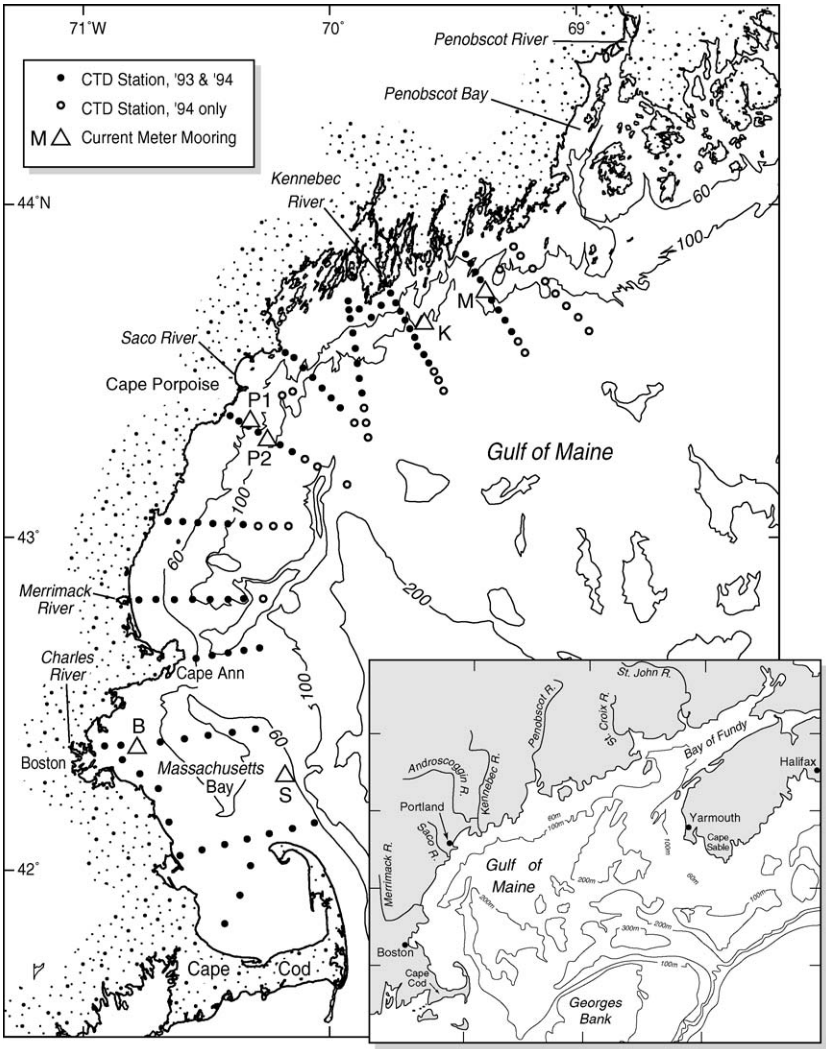

Fig. 1. Map of the western Gulf of Maine, showing the mooring locations, hydrographic stations and the mouths of major rivers.

packs of the Seabird sensors. A correction of 25° clockwise rotation was performed on all of the near-surface current data. This correction yields results that are consistent with the Ekman and geostrophic forcing conditions and are also consistent with subsequent observations (unpublished data) at the same location that reveal no significant offshore veering of the near-surface currents. This correction only has a minor (10%) influence on the magnitude of the along-shelf currents, but it has a dominant influence on the estimates of offshore velocities. Because of the uncertainty of the corrections, the estimates of the offshore component of the flow should be treated with caution. This paper focuses mainly on the along-shelf component of the flow.

2.2. Hydrography

Five large-scale hydrographic surveys were conducted in 1993 and three in 1994, each of which included 11 cross-shore lines along a 250-km portion of the western Gulf of Maine (Fig. 1). Additional surveys were conducted along the Cape

Porpoise transect. Most of the surveys were conducted on the R/V *ARGO* Maine, using a Neil Brown Mk III conductivity–temperature–depth instrument (CTD), and several surveys were conducted on the R/V *Anderson*, using a Seabird SBE-6 CTD. Beam attenuation and fluorescence were also measured by the CTD, and water samples were obtained at 6 depths at each station for nutrients and dinoflagellate cell counts (not discussed in this paper). The cross-shore spacing of stations was typically 3–5 km, and the along-shore separation of the lines was 20–30 km. Additional surveys over portions of the domain were performed intermittently during the two spring periods.

2.3. Drifters

Near-surface drifters were released near the mouth of the Kennebec River in conjunction with the shipboard observations. Releases were performed April 14, May 11 and May 25, 1993, and April 22, May 1, May 31 and June 3, 1994. The drifters were the crossed-vane, surface-following design as described by Davis (1985), except that they extended 2-m deep, to improve their tracking of the water relative to windage. They were tracked by ARGOS satellite, obtaining fixes 6–8 times per day, with accuracies of ± 300 m. The drifters had Falmouth Scientific inductive salinity sensors mid-way along the drogue at 1-m depth.

2.4. Other data

Meteorological data were obtained from the National Oceanographic and Atmospheric Administration (NOAA) meteorological buoy offshore of Portland, Maine. Wind speed was converted to wind stress using the quadratic drag formulation of Large and Pond (1981). The wind stress was rotated into along-coast and cross-coast directions, with the along-coast direction being 35° east of north. River discharge data were obtained from the US Geological Survey. The discharge values were adjusted to account for the drainage area downstream of the gauge sites.

3. Results

3.1. Time-series data

The time-variations of the forcing conditions and selected moored data are shown in Figs. 2 and 3, for the 1993 and 1994 observations, respectively. All of the data were filtered with a 35-h filter to remove tidal and other high-frequency fluctuations. (See below for a discussion of tidal motions.) The times of hydrographic surveys are indicated on the figures by vertical dotted lines.

The Western Maine river discharge was similar between the 2 years (Figs. 2 and 3, 1st panel.) In both years, the discharge peaked in mid-April, with the combined discharge exceeding 7000 $m^3 s^{-1}$ during the freshet period. The Kennebec–Androscoggin and Penobscot together accounted for more than 70% of the flow into the western Gulf. (The Androscoggin joins the Kennebec before it reaches the Gulf of Maine, so the discharges of the two rivers are considered together in this paper, and references to the Kennebec imply the confluent flow.) There were minor, subsequent peaks following the freshet in both years.

The wind stress is plotted on the 2nd panel as along-shore and cross-shore components (in the oceanographic, i.e., downwind, convention). The wind stress exhibited large fluctuations at time scales of 1–3 days and amplitudes of 0.1–0.2 Pa, with a small long-term mean. There was a downwelling-favorable wind event (negative, or southwestward stress) on April 13, 1993, at the time of the first hydrographic survey, and another on April 28, just before the second survey. However most of the wind events in 1993 were upwelling-favorable. 1994 had fewer distinctive events, although the statistics of the wind stress variability were comparable.

The time series of moored salinity along the Cape Porpoise transect clearly show the presence of the coastal current (Figs. 2 and 3, 3rd panel). In 1993, there was an abrupt onset of the coastal current at the P2 mooring about a week after the peak freshet in the Kennebec, and the near-surface salinity remained 2–3 psu below the ambient, deep

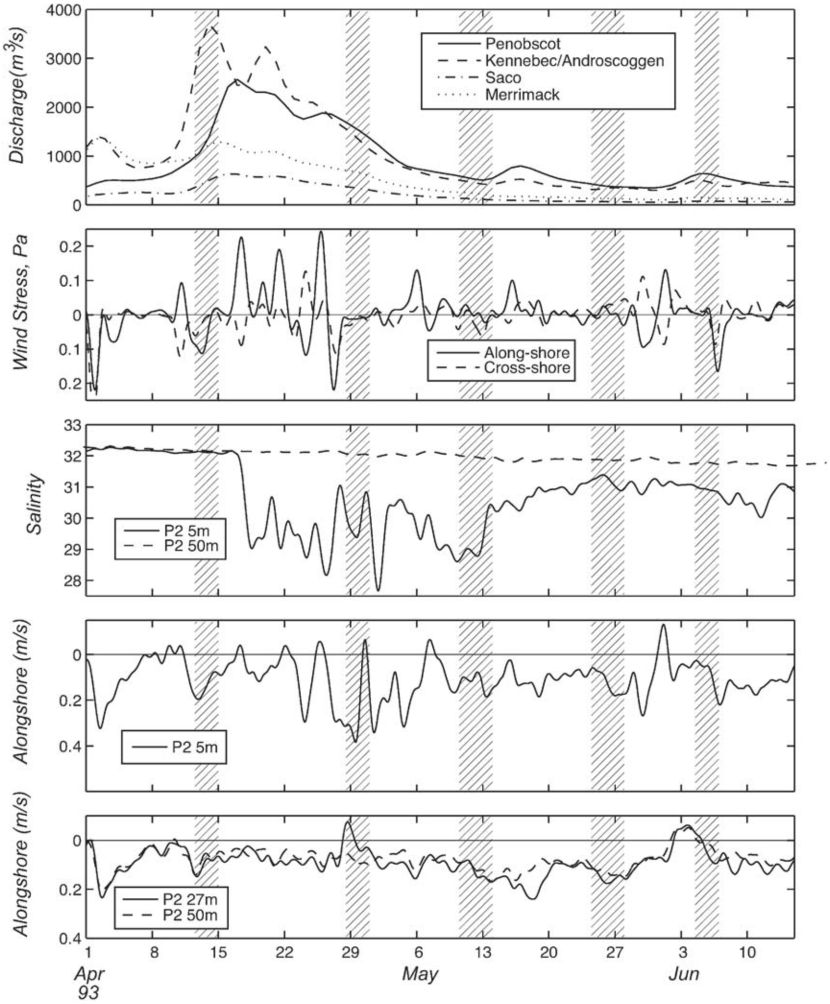

Fig. 2. Time-series data from the 1993 deployment period. Top panel: river discharge of the major rivers entering the western Gulf; 2nd panel: along-shore and cross-shore wind stress at the Portland meteorological buoy (positive values indicating wind blowing *toward* the northeast and southeast, respectively); 3rd panel: salinity at the P2 mooring; 4th panel: along-shore current at P2, 5-m depth; 5th panel: along-shore current at P2, 27- and 50-m depths. Wind, salinity and current data were low-pass filtered with a 35-h filter to remove tides and high-frequency fluctuations.

salinity for several weeks. The onset of the salinity signal at this mooring lagged the formation of the coastal current at the Cape Porpoise transect, as revealed by shipboard data obtained during the first cruise (see following section). The coastal current was confined to the waters inshore of the mooring until the upwelling wind event of April 18, which advected the plume past the mooring. During 1994, there was a more gradual onset of low salinity of the moorings, most likely because of several major upwelling wind events in early April. The salinity at the outer (P2) mooring increased abruptly around May 5, following a strong downwelling event. This is also consistent with the plume narrowing during downwelling conditions. Around May 21st, both moorings indicated salinity fluctuations that followed two modest downwelling-favorable wind events.

Salinity at 50-m depth showed a slow, seasonal decrease in both 1993 and 1994, dropping by

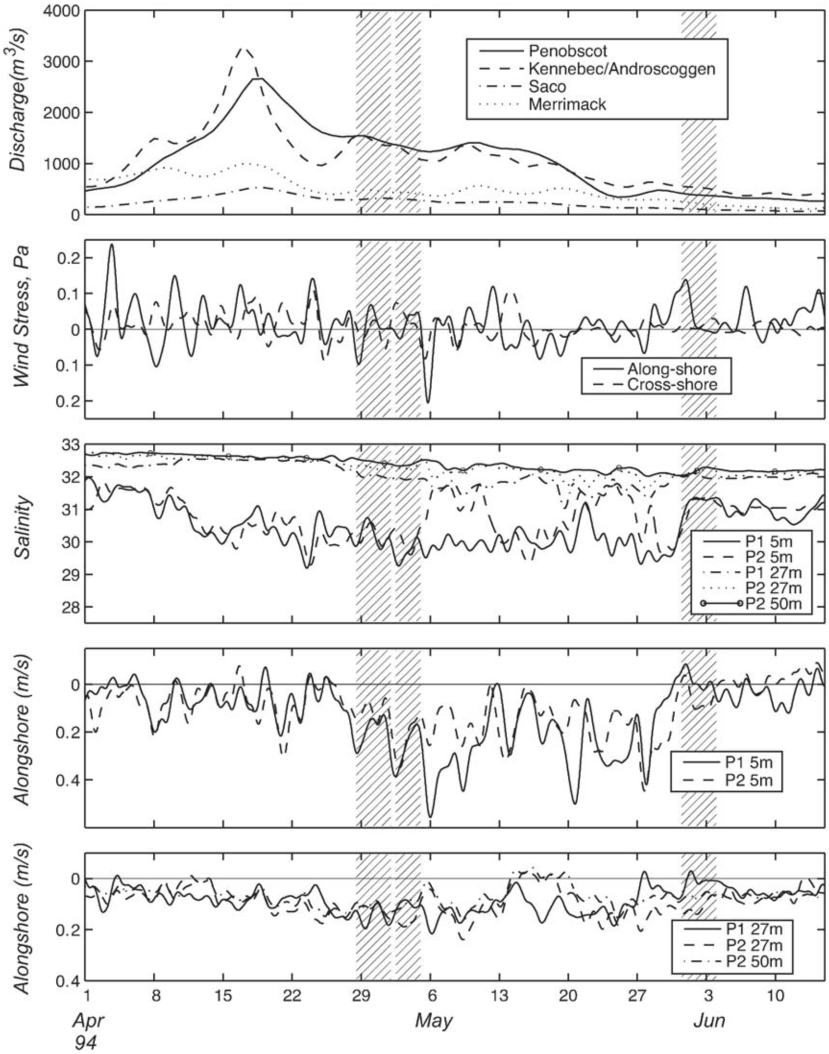

Fig. 3. Time-series data from the 1994 deployment period. Top panel: river discharge; 2nd panel: along-shore and cross-shore wind stress at the Portland meteorological buoy; 3rd panel: salinity at the P1 and P2 moorings; 4th panel: along-shore currents at near-surface instruments at P1 and P2; 5th panel: along-shore currents at deep instruments at P1 and P2.

about 0.5 psu over 2 months. This decrease did not appear to be correlated with any local forcing variables. The salinity at 27 m (1994 observations) often tracked the deep salinity, but there were several periods (typically following downwelling-favorable winds) when the 27-m salinity at the P1 mooring decreased, apparently due to deepening of the low-salinity layer.

Along-coast currents were directed generally down-coast (southwestward), both within and beneath the plume (Figs. 2 and 3, 4th and 5th panels). The signal of the coastal current was not as obvious as the salinity data due to the large influence of wind-driven fluctuations at 1–3 day time-scales, although there was enhanced southwestward flow in the near-surface waters during the April–May period of low surface salinities. The combination of low surface salinity and strong southwestward wind stress produced the strongest along-coast velocities (reaching $0.55\,\mathrm{m\,s^{-1}}$ on May

6, 1994). There were frequent reversals (positive along-shore component) of the surface current driven by northward wind-stress (e.g., late April, 1993), but these reversals tended to be short-lived and weak, even during strong wind events. Beneath the low-salinity surface layer, the flow was persistently southwestward, with velocities around 0.1 m s^{-1}.

Regression analysis was performed between salinity and velocity to assess the role of the freshwater signal in the velocity. The along-coast flow was weakly correlated with salinity variations ($r = 0.28$; significant at the 90% level), indicating higher along-shore currents when low-salinity water was present. There was a slight correlation between offshore flow and low salinity ($r = 0.30$; significant at the 90% level), indicating the influence of cross-shore advection. The small amount of velocity variance explained by the salinity is evidently due to the relatively strong wind-forced component of motion. Along-shore currents were correlated with both along-shelf and cross-shelf winds, with regression coefficients of 0.4–0.6. Cross-shore winds induced motion in the upper layer consistent with Ekman transport; along-shore winds drove surface currents in the same direction as the wind. (See discussion section for further analysis of wind-driven motions.)

Tidal velocities were generally weak: semi-diurnal tidal velocities at the Cape Porpoise moorings averaged 0.06–0.07 m s^{-1} over the deployment period. Tidal velocities were significantly stronger, about 0.3 m s^{-1}, at Mooring S near Massachusetts Bay. There were significant diurnal motions in the surface waters (0.03–0.07 m s^{-1}) that appeared to be driven by diurnal variations in wind stress, based on variations in amplitude of the diurnal winds and currents (Fig. 4). At the P1 mooring, the correlation was highly significant between the diurnal stress amplitude and the diurnal current amplitude ($r = 0.9$, significance $> 95\%$). The diurnal velocities were smaller in the deeper waters (0.02–0.03 m s^{-1}), with no apparent correlation with the winds. The wind-stress fluctuations were roughly aligned with the coast, as were the near-surface, diurnal current fluctuations. The excursions due to the semi-diurnal tides were approximately 1 km, and the excursions due to diurnal fluctuations were as much as 2 km (due to the longer period of the diurnal fluctuations).

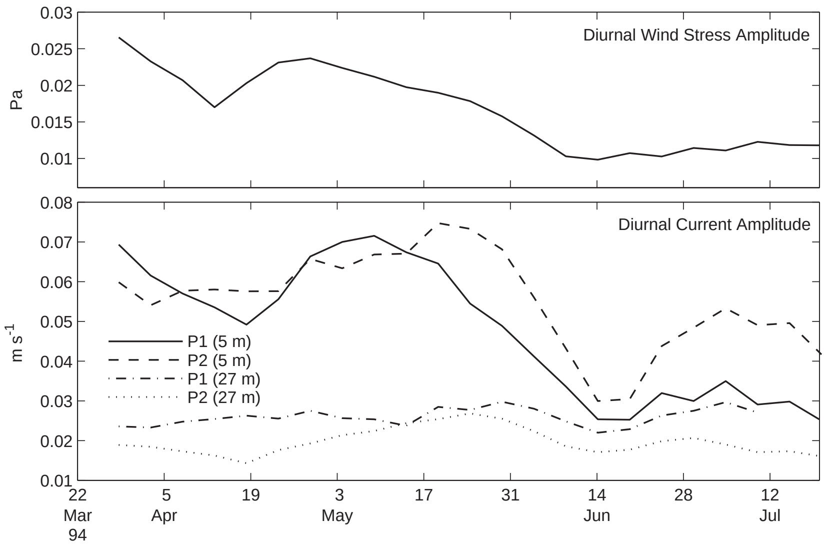

Fig. 4. Amplitude of diurnal fluctuations of wind stress (upper panel), and amplitude of diurnal velocity fluctuations at the Cape Porpoise moorings (second panel), based on 1994 observations. The tidal analysis was performed for 5-day segments in order to resolve the temporal variations of the fluctuations. The average orientation of the wind stress and current fluctuations was in the along-shore direction.

3.2. The spatial structure of the coastal current

The surface salinity distribution following the peak in river discharge in 1993 is shown in Fig. 5. This survey was conducted during the strongest near-surface, southwestward flow of the 1993 observations (Fig. 2, April 29), caused by the combination of downwelling-favorable winds and large freshwater input. A zone of low salinity extended 20–30 km from the coast and 250 km along the coast, from the mouth of Penobscot Bay into Massachusetts Bay. The lowest salinities (<28 psu) occurred to the south of the mouth of the Kennebec River, but the low salinities farther to the northeast suggest that the Penobscot River also contributed to the coastal current. Based on a typical vertical density distribution in the low-salinity zone, the internal deformation radius was 4–6 km. Thus, even during downwelling-favorable conditions, the plume was significantly wider than the deformation scale.

Near-Surface Salinity: April 28-30, 1993

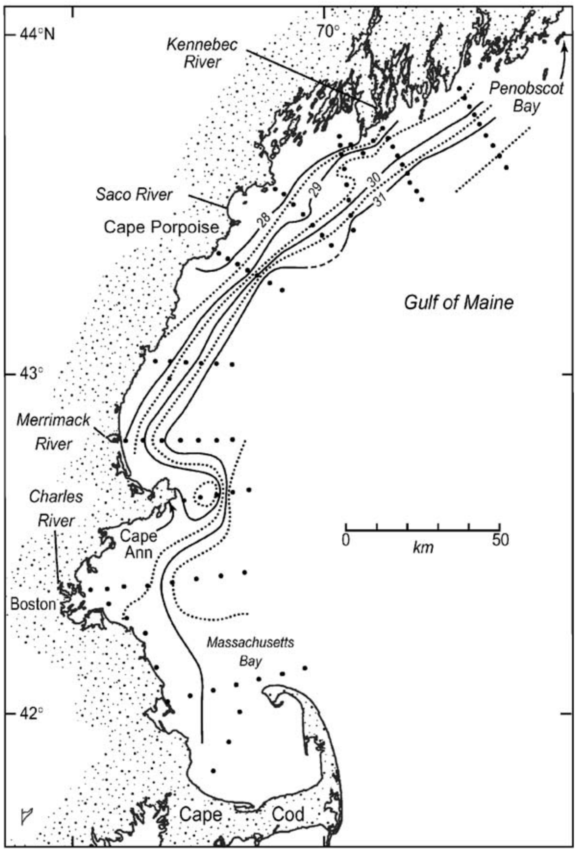

Fig. 5. Near-surface (2-m depth) salinity distribution during 1st large-scale hydrographic survey in 1993. Contour interval is 0.5 psu.

A plan view of the changes in the salinity field between April 29 and May 3, 1994 (Fig. 6) indicate that there are significant along-coast variations associated with changes in forcing conditions. The most pronounced difference between the two salinity distributions is the tongue of low-salinity water that showed up in the second survey, extending from the mouth of the Kennebec to the Cape Porpoise section. The origin of this low-salinity tongue appears to be the minor peak in discharge that occurred around April 29, accompanied by down-coast winds (Fig. 3). These conditions resulted in along-coast velocities of 0.2–0.4 $m\,s^{-1}$ in the plume, based on the moored data (Fig. 3). These speeds would result in displacements of 50 km in the 2.5 days separating the two cruises—enough to explain the 50-km long tongue of low-salinity water.

The width of the coastal current varied considerably between observations, due mostly to the influence of along-coast winds on the upwelling–downwelling regime (Fong et al., 1997). Several transects at the Cape Porpoise section during the 1993 and 1994 observations are shown in Fig. 7, illustrating the variations in offshore extent and structure of the plume. The upper panel shows the plume during the early part of the freshet in 1993, during downwelling conditions. The plume was only 10 km wide, and it extended to 25-m depth at the coast. Note that there was no signal of the plume at the P2 mooring at this time due to its narrowness. Two weeks later (second panel), the plume was 20 km wide and 20-m deep at the coast. This section corresponds to the plan view of Fig. 4. Downwelling conditions also occurred during this survey, although there were several strong upwelling events between the two surveys that may have caused the plume to spread seaward, in addition to a large addition of fresh water volume over the interval.

The 3rd and 4th panels clearly show the change in structure brought about by upwelling winds. The 3rd panel represents 1994 observations during

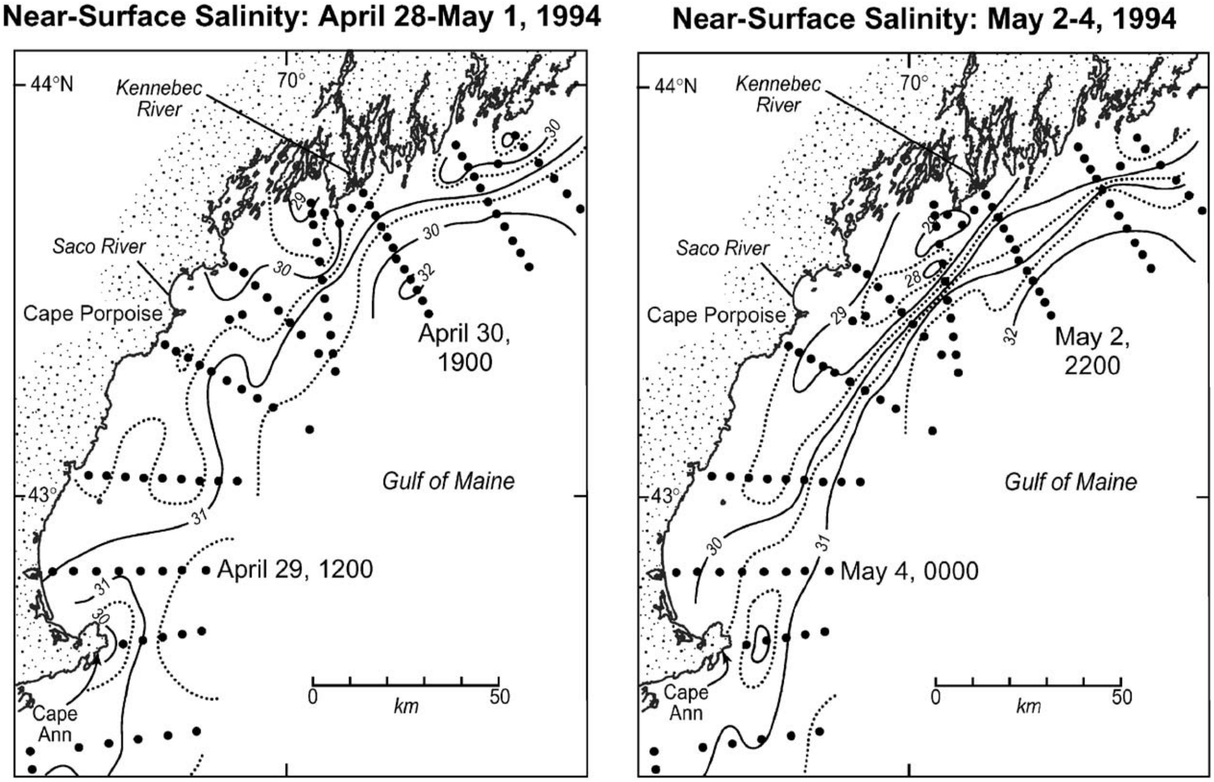

(A) (B)

Fig. 6. Near-surface (2-m depth) salinity distribution during two surveys in 1994, separated by several days. Dates and times that the ship occupied certain lines are indicated.

similar conditions as the 2nd panel: downwelling-favorable winds following the peak freshet. Around 1 May, the winds switched to upwelling-favorable, and the plume was advected an additional 12 km offshore. The cross-sectional area of the plume remained nearly the same during this upwelling event; the increased width was approximately balanced by the diminished thickness.

3.3. Drifter observations in the coastal current

Drifter trajectories from the 1993 and 1994 deployments are shown in Fig. 8. There were two types of trajectories, one in which the drifters traveled roughly parallel to the coast in the southerly direction, and the other in which the drifters followed a complex trajectory with relatively low velocities and no preferred along-coast motion. The two drifter trajectories from 1993 show the first type of trajectory, as do the first two from 1994. The latter drifters in 1994 show the second pattern. The along-coast trajectory occurred when the coastal current was well developed, and the other regime occurred when there was no longer a persistent southward flow along the coast (cf. Fig. 3). The drifters travelling within the coastal current had typical velocities of $0.15\,m\,s^{-1}$, occasionally exhibiting speeds in excess of $0.4\,m\,s^{-1}$. These speeds are similar to but usually slightly greater than the moored observations at 5-m depth, due to the shallower depth (and thus higher velocities) of the drogues at 0–2 m. One example of a rapid drifter trajectory is the drifter deployed on May 1,1994, corresponding to the hydrographic surveys shown in Fig. 6. This drifter traveled more than 40 km during one 24-h

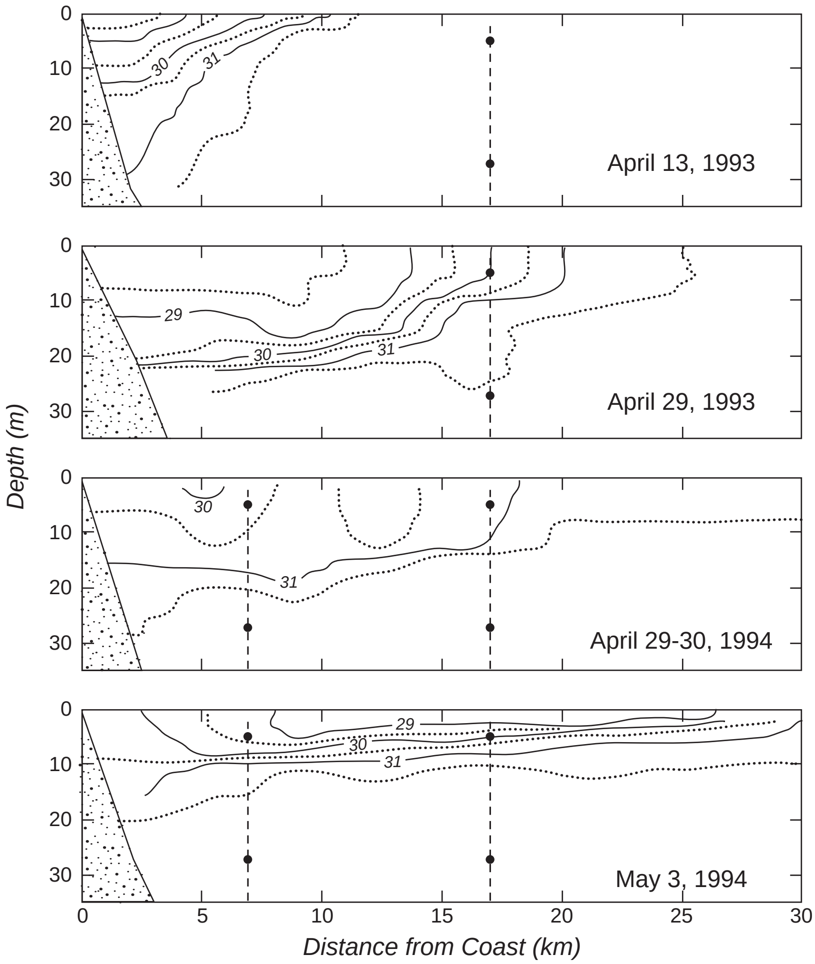

Fig. 7. Cross-shelf sections of salinity at the Cape Porpoise section during selected surveys in 1993 and 1994. Contour interval is 0.5 psu. The mooring locations are shown by vertical dashed lines.

period around May 5, under the influence of strong downwelling-favorable winds.

4. Discussion

4.1. Characteristics of the buoyant outflow

Following Garvine (1995, 1999), the general characteristics of the coastal current can be described by certain key parameters. The horizontal scales are normalized by the deformation radius

$$L_D = (g' h_c)^{1/2}/f,$$

where $g' = g(\rho_c - \rho_0)/\rho_0$ is the "reduced" gravity, with ρ_c the density within the coastal current, ρ_0 the density of the ambient water, g the acceleration of gravity, h_c the thickness of the coastal current, and f the Coriolis parameter. The "bulk" Kelvin number (Garvine, 1999) defines the non-dimensional width of the coastal current (or the relative importance of rotational processes to inertia)

$$K = L_c/L_D,$$

where L_c is the width of the coastal current. The mouth Kelvin number is similarly defined

$$K_m = L_m/L_D,$$

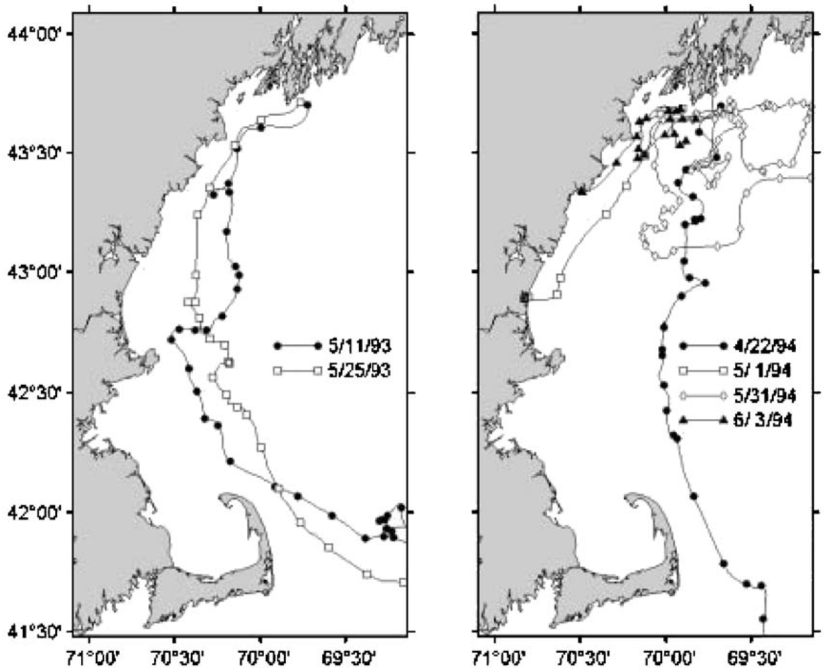

Fig. 8. Drifter trajectories during 1993 (left panel) and 1994 (right panel). The symbols are spaced by 24 h. The trajectories have been low-pass filtered to remove tidal and inertial motions.

where L_m is the width at the river mouth. The transport number T defines the ratio of the total freshwater transport to that which can be transported baroclinically by the coastal current. It is defined as

$$T = \frac{2Q_R s_0 f}{(s_c - s_0)g' h_c^2},$$

where Q_R is the total freshwater discharge, s_c and s_0 are coastal current and ambient salinities. Note that the inclusion of the ratio $s_0/(s_c - s_0)$ is a modification from Garvine (1999), to account for the dilution of the riverine water being transported by the coastal current.

The Froude number is the ratio of the current speed to the internal wave propagation speed, defined by

$$F = u_c/(g' h_c)^{1/2},$$

where u_c is a typical velocity within the coastal current.

The values of the key parameters for the western Maine coastal current are shown in Table 1. The bulk Kelvin number greater than 1 puts the western Maine coastal current in the "large-scale discharge" category of Garvine's (1995) classification scheme. It is close, in fact, to the value of the Delaware plume. The small value of K_m would suggest that the conditions at the mouth are strongly nonlinear and are likely to lead to the formation of a bulge (Garvine, 1999; Fong and Geyer, 2002). However, no bulge was evident in the hydrographic surveys. This may be in part the result of moderate ambient currents, which reduce the size of the bulge (Fong and Geyer, 2002), or perhaps tidal mixing near the mouth of the Kennebec River prevented bulge formation.

The value of T exceeding 1 is interesting, because it indicates that the freshwater inflow exceeds that which can be carried baroclinically by the coastal current. This deficit is apparently compensated by the barotropic component of flow, which augments the total transport, as discussed below.

Table 1
Key parameters of coastal current

Symbol	Parameter	Value
s_c	Coastal current salinity	29–30
s_0	Ambient salinity	32–32.5
h_c	Average thickness of coastal current	15 m
f	Coriolis parameter	$1 \times 10^{-4}\,s^{-1}$
L_D	Deformation scale	5 km
L_c	Width of coastal current	10 km (downwelling) 30 km (upwelling)
L_m	Width of mouth	0.5 km
u_c	Velocity in plume	0.2–0.4 $m\,s^{-1}$
Q_R	Typical freshwater discharge	3,000 $m^3\,s^{-1}$
K	Bulk Kelvin number	2 (downwelling) 6 (upwelling)
K_m	Mouth Kelvin number	0.1
T	Transport number	1.7
F	Froude number	0.4–0.8

4.2. Forcing variables of the coastal current

There are three main forcing variables for the coastal current: a barotropic pressure gradient that drives a depth-mean flow, a baroclinic pressure gradient that drives the vertically sheared velocity within the plume, and Ekman transport due to cross-shelf wind stress. Note that along-shelf wind stress contributes to the motion of the coastal current via its influence on the pressure gradient (Csanady, 1977). The relative contributions of these three factors was determined from analysis of the moored data at the Cape Porpoise section.

4.2.1. Barotropic motion

The barotropic flow was evident from the persistent along-shore flow beneath the plume, in waters of nearly uniform salinity, as indicated by time series data in 1994 (Fig. 3). The mean velocity beneath the plume at the Cape Porpoise section was 0.07–0.09 $m\,s^{-1}$, and similar velocities were found at the northern and southern moorings. This persistent, along-shore flow is most likely a manifestation of the large-scale, cyclonic circulation of the Gulf of Maine (Brown and Irish, 1992; Bigelow, 1927). There was a small contribution of wind forcing of the sub-plume motion (approximately 10% of the variance, based on linear correlation analysis), which was most evident at P1 at 27-m depth. This wind-forced motion was consistent with the barotropic response to along-shore winds (Csanady, 1977) associated with the set-up or set-down of sea-level.

4.2.2. Baroclinic motion

There was a pronounced, cross-shore salinity gradient during most of the hydrographic surveys, which produces a southwestward motion in the upper water column relative to the sub-plume waters, based on a geostrophic balance of the cross-shelf momentum equation. (Temperature gradients had a modest effect on density during the observation period.) The average contribution of the baroclinic shears to the down-coast velocity was 0.06 $m\,s^{-1}$ ($\pm$0.03 $m\,s^{-1}$ standard deviation), based on cross-sectional averages of all the hydrographic observations between the mouth of the Kennebec and the Cape Porpoise mooring array in 1993 and 1994. Thus the total contribution of the baroclinic shears to the down-coast motion was comparable, but slightly weaker, than the underlying barotropic motion. There were localized peak velocities of more than 0.40 $m\,s^{-1}$ associated with intensified transverse gradients, but on average the baroclinic contribution to the flow was smaller than the barotropic component of down-coast flow.

4.2.3. Wind-driven motions

The analysis of the wind-driven response was divided into along- and cross-coast components, to determine whether there was a difference in response to the two modes of forcing. For both along- and across-shore forcing, there was a strong response of the near-surface (5 m) currents, with transfer coefficients of 0.8–1.5 $\mathrm{m\,s^{-1}\,Pa^{-1}}$ wind stress. This is consistent with an Ekman layer thickness of 6.5–12.5 m, which is the same order as the plume thickness. The veering angles at the Kennebec and Cape Porpoise moorings were 25–46° clockwise relative to the along-shore component of wind stress, indicating the contributions of both Ekman veering and induced geostrophic motion. These veering angles are similar to those observed by Munchow and Chant (2000) in the Delaware Coastal Current. The veering angle of nearly 90° at Mooring S indicates the absence of geostrophic response, consistent with the lack of a coastal boundary.

Correlations were weak for the deeper measurements at P2, but there were significant wind-driven motions at the 27-m instrument at P1. The sense of this motion was consistent with upwelling–downwelling dynamics for the along-coast winds, i.e., the flow had an along-coast component and a cross-shore component due to the bottom Ekman veering. For cross-shelf winds, the deep flow was opposite the near-surface Ekman transport, with about one-third the magnitude.

The wind-driven component of flow was a major source of variance, particularly at the 1–3 day time scale of wind-forcing. Over time scales of a month, the variations in along-shore shear were consistent with the sense of the wind stress variations. However, the magnitude of wind stress variations on these time scales was far too small to account for the magnitude of variation in the along-coast shear, at least according to the linear regression analysis. The net reversal of shear during upwelling periods may indicate that linear regression underestimates the influence of wind stress, i.e., that nonlinear interactions between the wind stress and the plume motion may preferentially amplify the northeastward motions. One nonlinear effect is the wind-induced variation of plume thickness, and thus Ekman depth. If the Ekman depth were smaller during upwelling events, the flow would be rectified in the upwelling-favorable direction, even with oscillatory wind stress. Unfortunately, there was not enough vertical resolution in the moored data to quantify the time variations in plume thickness, so this hypothesis cannot be verified with these observations.

In summary, the barotropic motions, baroclinic shears, and wind-driven motions all have comparable and significant effects on the along-coast motion of the plume. In 1994, when the moored observations best resolved the plume, the barotropic component appeared to be the most important contributor to the mean, southwestward motion, and the month-to-month fluctuations were caused by variations in the relative contributions of baroclinicity and wind stress. The wind stress dominated the forcing at short time scales (1–2 days), but the longer-time scale variability was not simply related to either baroclinicity or wind stress.

4.3. Freshwater transport in the coastal current: Cape Porpoise transect

The transport in the western Maine coastal current was estimated at the Cape Porpoise transect for the 1994 observation period, in order to compare this transport with the riverine freshwater input and to assess its variability. The 1994 period was selected because two moorings were deployed along the Cape Porpoise transect, and there were 7 hydrographic surveys along that line over the course of the freshet period. The single mooring in 1993 was not adequate for transport estimates, because the coastal current was sometimes completely inshore of the mooring location.

An estimate of the freshwater flux requires an integral over the cross-section of the product of the salinity anomaly and the velocity:

$$Q_f = \iint u(y,z)\frac{(s_0 - s(y,z))}{s_0}\,\mathrm{d}y\,\mathrm{d}z, \qquad (1)$$

where $u(y,z)$ is the along-shelf velocity, s_0 is the ambient salinity outside the coastal current, $s(y,z)$ is the salinity within the coastal current, y is the cross-shore coordinate, and z is the vertical coordinate. The value of s_0 was determined from the salinity at 50-m depth at the Kennebec mooring, which was assumed to be below the influence of the local freshwater sources.

Two methods were used to estimate the other terms in the transport calculation, one using the hydrographic data during the individual cruises and the other using the continuous moored data from the Cape Porpoise line during 1994. The hydrographic data were used to obtain geostrophic estimates of the currents within the plume, integrating from 27-m depth to the surface. The velocity at 27-m was based on the average of the velocities at that depth at the two Cape Porpoise moorings (Fig. 3, bottom panel). The transport was then integrated from 27 m to the surface. Not including the contributions to flux deeper than 27 m might have slightly underestimated the plume transport, but it eliminated the spurious contribution from temporal variations in the deep (50 m) salinity. The geostrophic calculations generally agreed within $0.05\,\mathrm{m\,s^{-1}}$ with the 5-m currents, with one exception being the transect on May 2, 1994, in which the measured velocity exceeded the geostrophic estimate by $0.15\,\mathrm{m\,s^{-1}}$. This discrepancy is possibly explained by along-shelf Ekman transport due to moderate cross-shore winds at that time.

The mooring data provided continuous measures of the velocity and salinity within the plume, but they provided limited resolution of the vertical and cross-shore variability. However, the major fluctuations in the width and depth of the plume were associated with upwelling and downwelling, for which the changes in depth were inversely correlated with changes in width (cf., Fig. 6, 3rd and 4th panels). Thus, the area of the plume did not vary by nearly as much as either its depth or its width. A crude estimate of the along-shelf freshwater transport was performed by assuming that the plume had an area of $2\times10^5\,\mathrm{m}$ (e.g., 10-m deep and 20-km wide) at the Cape Porpoise section, and that the salinity and velocity within the plume could be represented by the measurements at the upper (5 m) moored instruments at P1 and P2. Comparison of freshwater transport estimates based on these assumptions with estimates using the complete hydrographic data along the Cape Porpoise section for 7 surveys in 1994 indicated that 75% of the variance was represented by the simplified estimate. Although not as accurate for individual surveys as the integral using the hydrographic data, the simplified approach provides a continuous time series for the entire moored deployment.

The estimated freshwater flux from the moored data is shown in Fig. 9, along with the estimates from the hydrographic surveys. The sum of the local riverine freshwater sources (Penobscot, Kennebec, Androscoggen, and Saco rivers) and the more distant St. John River discharge are also plotted. The seasonal variation of the freshwater flux is clearly evident; the transport increases sharply in early May, about 2 weeks after the peak riverine input. High freshwater transport continues through the month of May, abruptly ending in early June. The average freshwater transport past Cape Porpoise for the freshet period (March 21 to July 1) was $2800\,\mathrm{m^3\,s^{-1}}$. The integrated inputs from the local rivers was $1900\,\mathrm{m^3\,s^{-1}}$. Including the contribution of the St. John River, the freshwater input is $4100\,\mathrm{m^3\,s^{-1}}$. Thus the calculated transport in the coastal current is 30% larger than the local input estimate, and 30% smaller than the sum of all of the major rivers entering the Gulf. It is difficult to assess the magnitude of error in the transport calculation; most of the uncertainty is associated with estimating the distributions of salinity and velocity, which together could produce errors of 30%. Thus these transport estimates do not provide conclusive evidence for the contribution of the St. John River to the western Maine coastal current, but they are strongly suggestive.

The distance from the mouths of the major rivers to the observation location at Cape Porpoise should result in significant lags in the freshwater signal, which may be evident in the low-frequency (5 day filtered) variations of transport. The Cape Porpoise transect is approximately 80 km from the mouth of the Kennebec, 180 km from the mouth of the Penobscot River, and 500 km from the mouth of the St. Johns. The average speed within the plume during the month of May, when the coastal current was fully developed, was $0.21\,\mathrm{m\,s^{-1}}$, based on the 5-m current meters on the Cape Porpoise transect. If the freshwater signal moved through

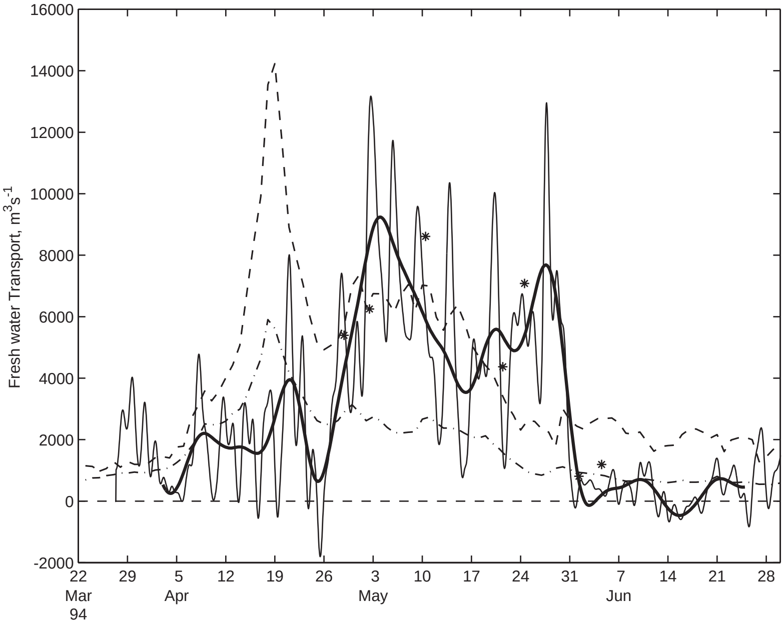

Fig. 9. Freshwater transport estimates based on moored and shipboard data during 1994. The thin solid line is the 35-h-filtered estimate of freshwater transport at the Cape Porpoise section. The heavy line is a 5-day-filtered estimate that removes the short-lived meteorological fluctuations. The asterisks are estimates of flux from shipboard measurements. The dash-dotted line is the combined freshwater input from the western Maine rivers, and the dashed line is the sum of those rivers plus the St. John River.

the entire Gulf at this propagation speed, the lag would be 4, 10 and 28 days from the Kennebec, Penobscot and St. John Rivers, respectively. The variations in freshwater transport are roughly consistent with these lags—there are transport maxima 3 and 15 days after the peak freshet, and there is a broad maximum from 30 to 40 days after the peak. The first two may be associated with the Kennebec and Penobscot inputs, and the third may be due to the more remote contributions from the St. John River. The Scotian shelf also contributes fresh water to the EMCC (Brooks, 1985; Pettigrew et al., 1998). However, the salinity of the Scotian shelf water is generally too high to contribute to the observed near-surface transport; rather it would contribute to the transport of the deeper water of 32–32.5 psu.

The contribution of the St. John has not been previously documented in the western Gulf, although the continuity of this transport was not ruled out by Brooks (1985) or Pettigrew et al. (1998). The freshwater transport calculations suggest that in 1994, more than half of the St. John discharge was transported into the western Gulf at salinities less than 32.5 psu, thus contributing a major fraction of the freshwater volume input to the western Gulf in 1994. The continuity of transport may vary considerably from year to year, due to differences in wind forcing during the time of maximum freshwater transport. There may also be interannual differences in the regional, Gulf of Maine circulation that influence the continuation of the EMCC transport into the western Gulf (Hetland, 1997).

Superimposed on this seasonal trend in freshwater transport are large fluctuations associated with wind forcing. The low-frequency wind stress was significantly correlated with fluctuations in freshwater transport ($r = 0.45$, significant at 95% level). The maximum transport occurred with northwesterly winds, which forced both downwelling and along-shore Ekman transport within the plume. Upwelling events, such as the large event in late April, could temporarily arrest or reverse the transport in the coastal current. An upwelling event in the beginning of June not only arrested the transport for the duration of the event, it appears to have terminated the alongshore transport of fresh water. It is conceivable that the mixing associated with the upwelling event weakened the density anomaly enough that the coastal current lost its coherence after this point in time. Following this event there were no significant downwelling events, which may be necessary to re-establish the coastal current structure.

4.4. Along-coast variability in freshwater transport

The along-coast variation in freshwater transport was difficult to quantify, due to the limited measurements of barotropic transport. However, the baroclinic component was readily determined from the hydrographic data. A reference level of 27 m was chosen to include virtually all of the baroclinic gradient associated with the salinity anomaly. Note that the total freshwater transport was significantly augmented by the southward flow measured at the 27-m depth, but this calculation provides an assessment of the along-coast variability of only the baroclinic part of the transport. Fig. 10 shows the baroclinic transport at 11 along-coast positions for all of the 1993 and 1994 large-scale surveys. There is a large amount of variability at each section due to seasonal changes and wind forcing, but there is a distinct along-coast

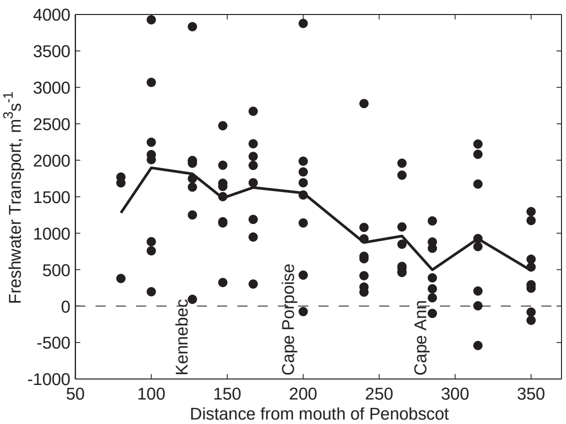

Fig. 10. Estimates of baroclinic freshwater transport from the large-scale hydrographic cruises in 1993 and 1994 plotted as a function of along-shore position. The scatter is largely due to meteorological fluctuations. The decreasing trend in transport is significant at greater than 95% confidence level.

variation in the time-averaged transport (solid line). It shows a peak near the mouth of the Kennebec, with a marked decrease in the south-westward direction of more than $1000\,m^3\,s^{-1}$. At the Cape Porpoise line the baroclinic transport is roughly half of the freshwater transported calculated from the moored data in 1994, indicating the large contribution of the barotropic flow at that section. It is possible that the southward reduction in baroclinic transport is compensated by an increase in barotropic flow. For example an increase of $0.05\,m\,s^{-1}$ between Cape Porpoise and Cape Ann would be enough to compensate for the decrease in the baroclinic component. However, it is also plausible that there was a significant offshore component of freshwater transport, which could account for the reduction in the along-shore component. An average offshore flow of approximately $0.02\,m\,s^{-1}$ within the plume would balance the apparent reduction of $1000\,m^3\,s^{-1}$. This magnitude is too small to determine definitively from the current meters, given the uncertainty of specifying the cross-shore direction. Offshore transport of fresh water is, however, suggested by the hydrographic data: the later surveys during both 1993 and 1994 indicate offshore spreading of the plume as it extended along the coast.

The approximate e-folding scale of the transport in the coastal current (i.e., the distance over which the baroclinic transport decreases by e^{-1}) is roughly 250 km. This length scale is probably a strong function of the geometry of the shoreline and the circulation of the Gulf of Maine. Interestingly, the largest decrease occurs between Cape Porpoise and Cape Ann, a region of relatively uniform coastal geometry. If a similar "leakage" of fresh water occurred along the Eastern Maine coastal current, then a much smaller contribution would have been expected from the fresh water of the St. John River than was suggested by the transport data. These data thus present an ambiguous picture of the coherence of the along-coast transport of fresh water. The large along-coast scale of the coastal current is consistent with observations of other river outflows (e.g., Garvine 1999 and references therein). The along-shelf variation in transport implied by the baroclinic calculations indicates, however, that significant along-shelf attenuation of the transport can occur at spatial scales of 50 km or less.

5. Summary and conclusions

The observations during freshet periods for 2 years in the western Gulf of Maine indicate a coastal current that has strong along-coast transport for approximately a month following the spring freshet. Salinity anomalies within the plume approach 10 psu near the mouth during high discharge periods, but more typically there is a 2 psu anomaly within the plume. The structure of the plume is strongly influenced at short time scales by fluctuations in wind stress; however the wind stress is not a dominant contributor to the net transport of the plume due to the small value of the seasonally averaged wind stress. A persistent, along-coast, barotropic current is the biggest contributor to the plume transport, exceeding the contribution of the baroclinic flow due to the density anomaly of the plume itself.

During the observations in 1994, the freshwater transport in the coastal current exceeded the freshwater discharge of the rivers feeding the western Gulf of Maine, suggesting that the larger discharge from the St. John River in the eastern Gulf may have also contributed to the coastal current. This contribution would suggest that the coastal current extended 500 km northeastward along the Gulf of Maine to the Bay of Fundy, implying a continuity between the coastal currents in the eastern and western Gulf. These observations also indicate a significant, along-coast reduction in the baroclinic transport as the coastal current extends southwestward along the western Gulf. This may indicate "leakage" of roughly a third of the low-salinity water in the seaward direction, or it may reflect an along-shelf change in the strength of the barotropic flow.

Acknowledgements

This effort was supported in part by the US ECOHAB Program sponsored by NOAA, the US EPA, NSF, NASA and ONR, under NSF Grant OCE-9808173 and NOAA Grant NA960P00pp, and in part by NOAA Grant NA36RM0190 through the Gulf of Maine Regional Marine Research Program. The views expressed herein are those of the author(s) and do not necessarily reflect the views of NOAA or any of its subagencies. This is the contribution number 10712 from the Woods Hole Oceanographic Institution and the publication number from the ECOHAB program is 85.

References

Bigelow, H.B., 1927. Physical oceanography of the Gulf of Maine. Bulletin of US Bureau of Fisheries 40, 511–1027.

Brooks, D.A., 1985. Vernal circulation in the Gulf of Maine. Journal of Geophysical Research 90, 4687–4705.

Brown, W.S., Irish, J.D., 1992. The annual evolution of geostrophic flow in the Gulf of Maine: 1986–1987. Journal of Physical Oceanography 22, 445–473.

Chao, S.-Y., 1988. Wind-driven motion of estuarine plumes. Journal of Physical Oceanography 18, 1144–1166.

Chao, S.-Y., Boicourt, W.C., 1986. Onset of estuarine plumes. Journal of Physical Oceanography 16, 2137–2149.

Chapman, D.C., Barth, J.A., Beardsley, R.C., 1986. On the continuity of mean flow between the Scotian Shelf and the Middle Atlantic Bight. Journal of Physical Oceanography 16, 758–772.

Csanady, G.T., 1977. Intermittent full upwelling in Lake Ontario. Journal of Geophysical Research 82, 397–419.

Davis, R.E., 1985. Drifter observations of coastal surface currents during CODE: the method and descriptive view. Journal of Geophysical Research 90 (C3), 4741–4755.

Dinnel, S.P., Wiseman Jr., W.J., 1986. Fresh water on the Louisiana and Texas shelf. Continental Shelf Research 6, 765–784.

Fong, D.A., Geyer, W.R., 2002. The alongshore transport of freshwater in a surface-trapped river plume. Journal of Physical Oceanography 32, 957–972.

Fong, D.A., Geyer, W.R., Signell, R.P., 1997. The wind-forced response of a buoyant coastal current: observations of the western Gulf of Maine plume. Journal of Marine Systems 12, 69–81.

Franks, P.J.S., Anderson, D.M., 1992. Alongshore transport of a toxic phytoplankton bloom in a buoyancy current: *Alexandrium tamarense* in the Gulf of Maine. Marine Biology 112, 153–164.

Garvine, R.W., 1974. Physical features of the Connecticut River outflow during high discharge. Journal of Geophysical Research 79 (6), 831–846.

Garvine, W.R., 1995. A dynamical system for classifying buoyant coastal discharges. Continental Shelf Research 15, 1583–1596.

Garvine, R.W., 1999. Penetration of buoyant coastal discharge onto the continental shelf: a numerical model experiment. Journal of Physical Oceanography 29, 1892–1909.

Hetland, R.D., 1997. The evolution of the vernal circulation in the Eastern Gulf of Maine. Masters Thesis, University of Maine, Orono, 98pp.

Hickey, B.M., Pietrafesa, L.J., Jay, D.A., Boicourt, W.C., 1998. The Columbia River plume study: subtidal variability in the velocity and salinity fields. Journal of Geophysical Research 103 (C5), 10339–10368.

Kourafalou, V.H., 1999. Process studies on the Po River plume, Northern Adriatic Sea. Journal of Geophysical Research 104, 29963–29985.

Kourafalou, V.H., Oey, L.-Y., Wang, J.D., Lee, T.N., 1996. The fate of river discharge on the continental shelf 1. Modeling the river plume and the inner shelf coastal current. Journal of Geophysical Research 101 (C2), 3435–3455.

Large, W.G., Pond, S., 1981. Open ocean momentum flux measurements in moderate to strong winds. Journal of Physical Oceanography 11, 324–336.

Lentz, S.J., Limeburner, R., 1995. The Amazon River plume during AMASSEDS: spatial characteristics and salinity variability. Journal of Geophysical Research 100, 2355–2375.

Lynch, D.R., Holboke, M.J., Naimie, C.E., 1997. The Maine coastal current: spring climatological circulation. Continental Shelf Research 17, 605–634.

Munchow, A., Garvine, R.W., 1993. Buoyancy and wind forcing of a coastal current. Journal of Marine Research 51, 293–322.

Nielsen, J.P., Higgins, W.B., Lippert, R.G., 1996. Water Resources Data for Maine, Water Year 1995, Report no. USGS/WDR/ME-95/1, Springfield, VA, United States, 200pp.

Oey, L.-Y., Mellor, G.L., 1993. Subtidal variability of estuarine outflow, plume, and coastal current: a model study. Journal of Physical Oceanography 23, 164–171.

Pettigrew, N.R., Townsend, D.W., Xue, H., Wallinga, J.P., Brickley, P.J., Hetland, R.D., 1998. Observations of the Eastern Maine Coastal Current and its offshore extensions in 1994. Journal of Geophysical Research 103, 30623–30639.